Dynamics of a One-Dimensional Array of Liquid Columns

F. Giorgiutti, A. Bleton, L. Limat, and J. E. Wesfreid

Laboratoire de Physique et de Mécanique des Milieux Hétérogènes (URA CNRS 857),
Ecole Supérieure de Physique et de Chimie Industrielles de la Ville de Paris,
10 rue Vauquelin, 75231 Paris Cedex 05, France

We study the instability induced by the gravity of a liquid layer hanging at the bottom of a horizontal cylinder and continuously supplied with "fresh" liquid. Depending on the flow rate, different regimes are observed: dripping, array of liquid columns, and liquid sheets. The column array exhibits collective behaviors that can be forced under well controlled conditions by driving the displacements of two boundary columns: optical mode (regular or "chaotic"), phase diffusion, and propagation of localized "dilation waves" of the pattern.

The falling of liquid from a solid ceiling is a fascinating phenomenon occurring in diverse situations such as waterfalls, fountains, and overflowing gutters. The involved free surface flows become important in many technical situations such as aerosol or fiber generation by centrifugal effects [1]. However, few studies have investigated the different flow regimes and the dynamics of the observed structures [2–5]. Pritchard [2] studied the pouring of a liquid at the lowest edge of an inclined plate. When the flow rate was increased, he observed successively three main regimes: (a) drop falling, (b) flow in liquid columns, and (c) liquid sheets. He gave a classification of numerous intermediate states and observed that the arrays of dripping sites as well as the arrays of liquid columns exhibited a well defined spatial periodicity. This somewhat striking order was reported in fact earlier by Lee [3] and by Carlomagno and de Luca [4] in the case of a horizontal cylindrical ceiling. They attributed this spatial periodicity to a Rayleigh-Taylor instability [5] of the film hanging below the solid ceiling, the influence of a possible Rayleigh instability becoming negligible for a sufficiently large cylinder radius.

These studies were mainly focused on the "static" properties of the observed structures. In this Letter we present a first study of the dynamics of the column array. As we suggested in a previous paper [5], this system constitutes an example of a one-dimensional cellular structure resulting from an instability [6]. These structures have been recently studied in diverse experiments such as directional solidification [7], directional viscous fingering ("printer's instability") [8], or other hydrodynamic instabilities [9] and still constitute an active field of research. Pictures of our experiment are reproduced in Fig. 1. In its simplest version [5], a horizontal hollow half cylinder is supplied with liquid at a constant rate Q by injectors distributed along the cylinder ("rain gutter" geometry). The liquid overflows, runs over the external sides, and accumulates below the cylinder where the instability occurs. For quantitative measurement, a better uniformity of the flow rate

was achieved (see Fig. 2) by feeding with liquid a hollow cylinder by its two extremities, the liquid being ultimately supplied along its upper side through a thin slot. Our experimental conditions were as follows: We used an aluminum cylinder of external radius $R_2 = 2.5$ cm, internal radius $R_1 = 2.0$ cm, and slot thickness 0.1 cm.
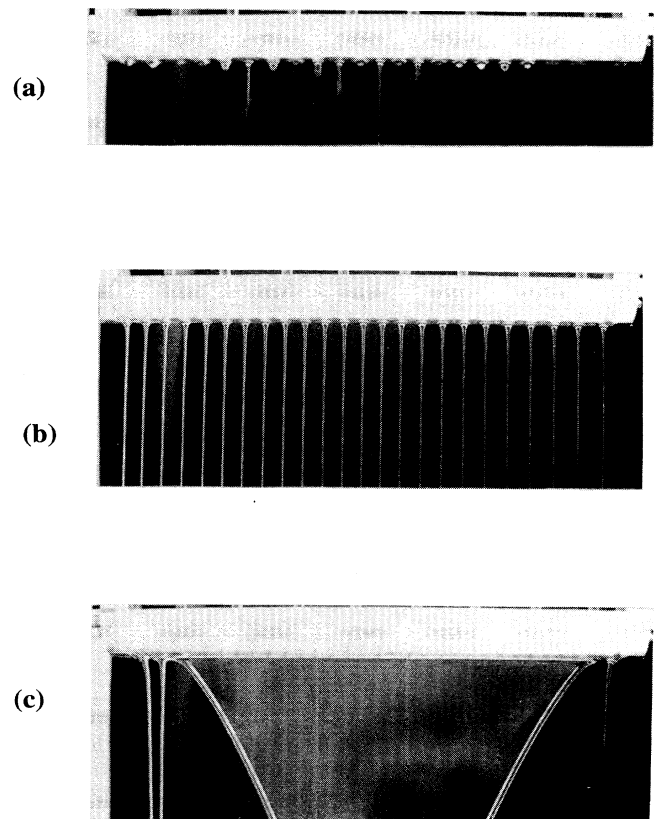

FIG. 1. Different regimes observed in our experiment: (a) array of dripping sites, (b) array of liquid columns, and (c) triangular liquid sheet.
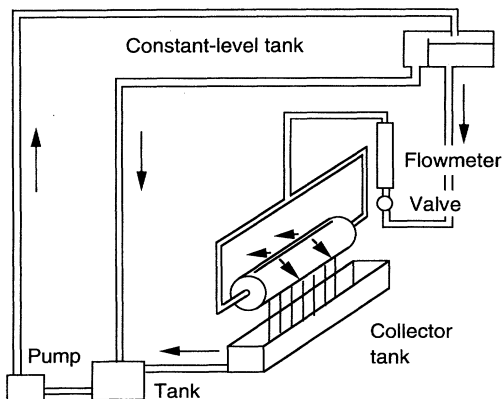
0031-9007/95/74(4)/538(4)$06.00

FIG. 2. Schematic experimental setup. The liquid is supplied through a thin slot at the top of the cylinder.

The liquid is a silicone oil (density $\rho = 0.97$ g/cm^3, viscosity $\eta = 20$ cP, and surface tension $\gamma = 21$ dyn/cm) that avoids dewetting effects. The total length available for the pouring of the liquid is $L = 28$ cm. A natural control parameter of the flow is given by the local flow rate q, defined as the flow rate per unit length of cylinder $q = Q/L$.

The array of dripping sites [Fig. 1(a)] is observed below a critical threshold for q, of order $q_{c1} \approx 0.1$ cm^2 s^{-1}. The drops exhibit a well defined spatial periodicity, the wavelength $\lambda_d = 1.30 \pm 0.05$ cm being close to that expected in the Rayleigh-Taylor instability of a thin layer [5],

$$\lambda_{RT} = 2\pi\sqrt{2\gamma/\rho g} \approx 1.32 \text{ cm}, \tag{1}$$

in which $g = 9.81$ m s^{-2} is the acceleration of gravity. Above q_{c1}, the array of dripping sites is gradually replaced by the column array [Fig. 1(b)]. The spatial periodicity of this system is also well defined, its wavelength $\lambda_{lc} = 1.20 \pm 0.05$ cm being independent of the flow rate q. Above a second threshold ($q_{c2} \approx 7.5$ cm^2 s^{-1}), the column array disappears and is replaced by liquid sheets [Fig. 1(c)].

A concept of central interest in the description of a cellular structure is the so-called "phase" variable [10], which can be identified with the local displacements of the cells divided by a reference value of the wavelength $\phi(x,t) = 2\pi u_x(x,t)/\lambda$. Its gradient $Q_\phi = \partial\phi/\partial x$ is equal to the local relative variation of wavelength $Q_\phi = \delta\lambda/\lambda$. For weak perturbations, it is know that the "phase dynamics" is governed by a diffusion equation in which the diffusion constant D is a function of the control parameter and of λ [10,11]. This equation has been extended by Coullet and Iooss [12] to the case in which the phase is coupled with the order parameter A of a secondary instability associated with a particular symmetry breaking. This theory allowed them to recover and classify very general mechanisms of wavelength selection.

Their equations read:

$$\frac{\partial\phi}{\partial t} = D\frac{\partial^2\phi}{\partial x^2} + f\left(A, \frac{\partial}{\partial x}\right), \tag{2a}$$

$$\tau_0\frac{\partial A}{\partial t} = (\mu - \mu_c)A + \gamma A\frac{\partial\phi}{\partial x} + g\left(A, \frac{\partial}{\partial x}, \ldots\right), \tag{2b}$$

where μ is the control parameter, μ_c is the threshold of the secondary instability, τ_0 and γ are constants, and f and g are nonlinear functions that depend on the nature of the broken symmetry. Usually the generation of these instabilities, as well as that of the Eckhaus instability ($D < 0$) [10] is forced by sudden variation of the control parameter μ. An alternative possibility would consist in applying a uniform strain to the structure associated with a large scale phase gradient $Q_\phi = \delta\lambda/\lambda = \partial\phi/\partial x$. Owing to the coupling between A and ϕ in Eq. (2b), the secondary instabilities could be forced under well defined conditions and quantitatively studied as a function of the forced spatial periodicity. We have realized this experiment in the case of the column array by using capillary effects: The position of a column can be forced by touching a column with a needle in contact with the bottom of the cylinder. Once this has been done, the center of the column remains always anchored to the needle and follows its possible displacements. A typical needle diameter was of order 0.3 mm, while that of a column is of order 1 mm. We have imposed strong boundary conditions by placing two needles in contact with the cylinder, at a given distance X from each other. For a given number of cells N, the wavelength $\lambda = X/N$ can be modified by slightly displacing one of the needles by means of a micrometer screw. Different phenomena were observed depending on the imposed value of λ. Below a first threshold ($\lambda < \lambda_1$ typically of order 1 cm), reorganizations occur by coalescence between columns. In the range $\lambda_1 < \lambda < \lambda_2$, λ_2 being a second threshold (typically of order 1.3 cm), the column array is stable. Above λ_2, a bifurcation toward an oscillatory state is observed: Each column oscillates as a whole, its motion being out of phase with that of its nearest neighbors. This "optical mode" is reminiscent of that observed in directional solidification and in the printer's instability [7,8]. We have followed this motion by recording a line of the digitized picture taken by a video camera and stored at constant time intervals. The line is horizontal and selected as close as possible to the bottom of the cylinder. This allows us to build spatiotemporal diagrams giving the $(x\text{-}t)$ trajectories of the columns. An example is given in Fig. 3(a) in the case of four oscillating columns. When the distance from the threshold is increased, the column oscillation evolves toward a transient "chaotic" behavior [Fig. 3(b)], followed by the nucleation of a new column after a variable time. As a result, the wavelength falls below λ_2, and the oscillations disappear. This forcing of a secondary bifurcation by explicit control of the
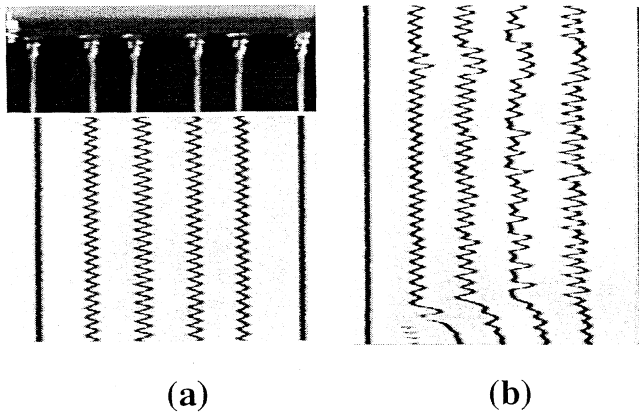
(a)   **(b)**

FIG. 3. (a) Oscillations of four columns. The mean wavelength λ is forced by the positions of the boundary columns. Time increases downward. (b) Chaotic oscillations observed after again increasing λ.

wavelength has been rarely achieved [13,14]. King and Swinney [13] were able to force transitions between different wavy vortex states in the Taylor-Couette system with a similar method.

We have quantified the occurrence of the optical mode by looking at the oscillations of one free column between two columns of fixed positions x_1 and x_2. The evolution of the amplitude $|A|$ and frequency ν of the oscillation as a function of the imposed "effective wavelength" $\lambda = (x_2 - x_1)/2$ is reproduced in Fig. 4. These points were obtained for a constant value of the local flow rate $q = 0.23$ cm^2 s^{-1}. By using appropriate lenses, we were able to measure $|A|$ and λ with an accuracy of order 0.005 cm. The frequency measurement is of order $\delta\nu/\nu = 1\%$. The
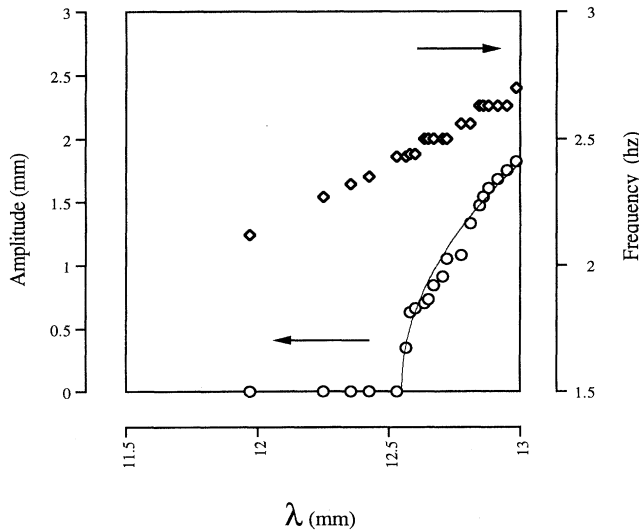

λ (mm)

FIG. 4. (a) Amplitude $|A|$ and frequency ν obtained for one free column oscillating between two columns of fixed position versus λ.

observed behavior is in good agreement with a model based on a supercritical Hopf bifurcation, governed by a complex Landau equation,

$$\tau_0 \frac{\partial A}{\partial t} = \varepsilon(1 + ic_0)A - g'(1 + ic_1)|A|^2 A, \quad (3)$$

in which A designates the amplitude of the oscillation and ε is the distance from threshold $\varepsilon = (\lambda - \lambda_2)/\lambda_2$. This quite unusual bifurcation parameter plays the role of $\partial\phi/\partial x$ in Eq. (2b). The time constant τ_0 and the constants g', c_0, and c_1 are usually deduced from the observed ε dependence of the saturated amplitude $|A| = \sqrt{\varepsilon/g'}$ and frequency $\nu = \nu_0 + (c_0 - c_1)\varepsilon/2\pi\tau_0$ of the oscillations above threshold (ν_0 is the frequency at threshold) and from a study of the linear relaxation oscillations below threshold. These relaxation oscillations are supposed to behave asymptotically as $\exp(-t/\tau)\exp(2i\pi\nu t)$ with $\tau = \tau_0/\varepsilon$ and $\nu = \nu_0 + c_0\varepsilon/2\pi\tau_0$. We then performed a second set of experiments, below the threshold, in which the central column was suddenly shifted from its equilibrium position. The relaxation oscillations were followed with spatiotemporal diagrams from which the value $\tau_0 = 0.062 \pm 0.003$ s was obtained. The measurement obtained for ν is available in Fig. 4 together with the best fit of the data that lead to the following values: $g' = 0.010 \pm 0.001$ mm^{-2}, $\nu_0 = 2.44 \pm 0.02$ Hz, and $c_0/2\pi\tau_0 \approx (c_0 - c_1)/2\pi\tau_0 = 7.15 \pm 0.15$ Hz. At the accuracy of our measurements the nonlinear contribution to the frequency appears to be negligible compared to the linear one, the coefficient c_1 being small compared to $c_0 = 1.63 \pm 0.06$.

After this first study of the array dynamics under stationary conditions, we have investigated its response to time-dependent perturbations. Our method was similar to that developed by other groups in earlier phase diffusion experiments [11]: The position of one of the boundary columns was fixed, and the other one oscillating according to $x = x_0\cos(2\pi ft)$. In practice, this was achieved by driving the needle motion with an x-t recorder excited by a function generator. An example of the spatiotemporal behavior obtained at "low" values of x_0 and f ($x_0 = 1.35$ cm and $f = 0.006$ Hz) is presented in Fig. 5(a). The local flow rate was set at the same value as before, $q = 0.23$ cm^2 s^{-1}. This picture reveals a phase diffusion mechanism in qualitative agreement with the diffusive limit of Eq. (2a). We have also quantitatively studied this phenomenon by trying to check the expected behavior for the spatiotemporal dependence of the phase $\Phi(x, t) = \alpha(x)\exp[2i\pi ft + i\psi(x)]$, where α and ψ designate, respectively, the local amplitude of the force oscillations and the local value of the temporal phase shift:

$$\alpha(x) = \alpha_0\exp\left(-\sqrt{\pi f/D}\,x\right), \quad (4a)$$

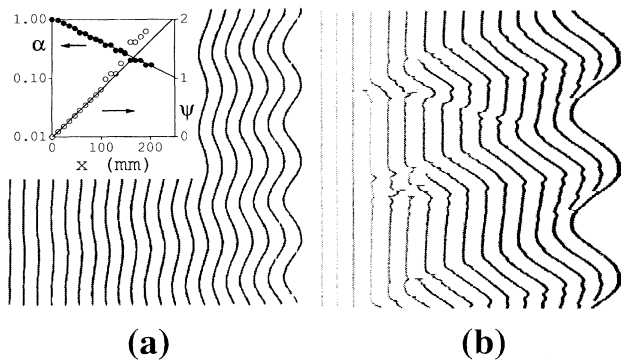$$\psi(x) = \sqrt{\pi f/D}\,x. \quad (4b)$$

(a)   **(b)**

FIG. 5. (a) Spatiotemporal behavior observed for $q = 0.23$ cm^2 s^{-1} with a moving boundary condition, following a sinusoidal law $x = x_0 \cos(2\pi ft)$ with $x_0 = 1.35$ cm and $f = 0.006$ Hz. Inset: spatial dependence of the forced amplitude and of the temporal phase shift. (b) Generation of dilation waves obtained for $x_0 = 3.23$ cm and $f = 0.15$ Hz.

The experimental variation of these two quantities has been plotted in Fig. 5(a). In both cases, the linear behavior is well recovered. These curves give two independent determinations of D in close agreement: $D_\alpha = 2.10 \pm 0.05$ cm^2 s^{-1} and $D_\psi = 1.95 \pm 0.10$ cm^2 s^{-1}. When one simultaneously varies x_0 and f, a rich variety of behaviors is observed: phase diffusion, periodic disappearance and nucleation of cells, local growth and diffusion of the optical mode, and also generation of "solitary" waves. An example of this last case is reproduced in Fig. 5(b). These waves in which a drift of the cells and the whole wave motion occur in opposite directions are reminiscent of the "dilation waves" observed in the printer's instability [8], and more generally in other one-dimensional systems [6,7]. The ratio of the drift velocity of the columns v_d to the "group" velocity v_g (velocity of the perturbation) was found to be nearly constant and independent of the flow rate q, $v_d/v_g = 0.35 \pm 0.05$. In addition, we have observed that the maximum speed of the needle $v = 2\pi f x_0$ must remain contained between two critical speeds v_{min} and v_{max}. Below v_{min}, the phase diffusion is observed, while above v_{max} the wavelength variations imposed by the boundary columns are compensated by nucleation or disappearance of cells. The two critical velocities were found to depend weakly on f and on the local flow rate q, remaining, however, of order $v_{min} = 1.5 \pm 0.5$ cm s^{-1} and $v_{max} = 8 \pm 3$ cm s^{-1} in the studied range ($f = 0.02-0.4$ Hz, $q = 2-4$ cm^2 s^{-1}).

In summary, we have investigated a new one-dimensionally extended dynamical system. This system is particularly well suited to studies of the phase dynamics under controlled conditions. In the case of an imposed constant wavelength dilation, we have pointed out a supercritical secondary bifurcation leading to an optical mode in which the motion of each column remains out of phase with that of its nearest neighbors. In the case of dynamical perturbations, a phase diffusion behavior

is observed at low frequency and is replaced by the generation of forced dilation waves when the forcing amplitude is increased.

[1] J. O. Hinze and H. Milborn, J. Appl. Mech. (1950); V. Sh. Zinatullin, A. E. Kulago, and V. P. Myasnikov, Sov. Phys. Dokl. **28**, 618 (1984).

[2] W. G. Pritchard, J. Fluid Mech. **165**, 1 (1986).

[3] S. L. Lee, J. Appl. Mech. **85**, 443 (1983).

[4] G. M. Carlomagno, in Proceedings of the Second AIMETA Congres, Napoli (Italy, 16–19 October 1974), p. 253; L. de Luca, Stab. App. Anal. Cont. Media (to be published).

[5] L. Limat, P. Jenffer, B. Dagens, E. Touron, M. Fermigier, and J. E. Wesfreid, Physica (Amsterdam) **61D**, 166 (1992).

[6] J. M. Flesselles, A. J. Simon, and A. J. Libchaber, Adv. Phys. **40**, 1 (1991).

[7] J. Bechhoefer, A. Simon, A. Libchaber, and P. Oswald, Phys. Rev. A **40**, 2042 (1989); G. Faivre, S. de Cheveigné, C. Guthman, and P. Kurowski, Europhys. Lett. **9**, 779 (1989).

[8] M. Rabaud, S. Michalland, and Y. Couder, Phys. Rev. Lett. **64**, 184 (1990); L. Pan and J. R. de Bruyn, Phys. Rev. Lett. **70**, 1791 (1993).

[9] F. Daviaud, M. Dubois, and P. Bergé, Europhys. Lett. **9**, 441 (1989); I. Mutabazi, J. J. Hegseth, C. D. Andereck, and J. E. Wesfreid, Phys. Rev. Lett. **64**, 1729 (1990); H. Willaime, O. Cardoso, and P. Tabeling, Phys. Rev. Lett. **67**, 3247 (1991).

[10] Y. Pomeau and P. Manneville, J. Phys. (Paris), Lett. **40**, L609 (1979); H. R. Brand, Prog. Theor. Phys. **71**, 1096 (1984); P. Manneville, *Dissipative Structures and Weak Turbulence* (Academic Press, New York, 1990).

[11] J. E. Wesfreid and V. Croquette, Phys. Rev. Lett. **45**, 634 (1980); M. Wu and C. Andereck, Phys. Rev. A **43**, 2074 (1991); L. Fourtune, W. J. Rappel, and M. Rabaud, Phys. Rev. E **49**, 3576 (1994).

[12] P. Coullet and G. Iooss, Phys. Rev. Lett. **64**, 866 (1990); see also F. Daviaud, J. Lega, P. Bergé, P. Coullet, and M. Dubois, Physica (Amsterdam) **55D**, 287 (1992), and S. Fauve, S. Douady, and O. Thual, J. Phys. II (France) **1**, 311 (1991).

[13] G. P. King and H. L. Swinney, Phys. Rev. A **27**, 1240 (1983).

[14] V. Croquette and F. Schossler, J. Phys. (Paris) **43**, 1183 (1982); M. Lowe and J. P. Gollub, Phys. Rev. Lett. **55**, 625 (1985); M. Boucif, J. E. Wesfreid, and E. Guyon, J. Phys. (Paris), Lett. **45**, 413 (1984).
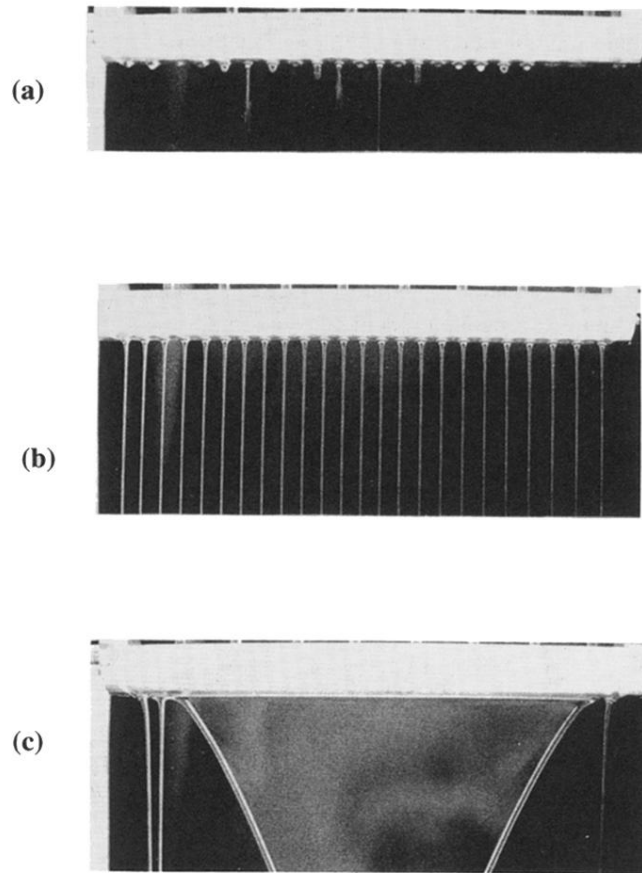
FIG. 1. Different regimes observed in our experiment: (a) array of dripping sites, (b) array of liquid columns, and (c) triangular liquid sheet.
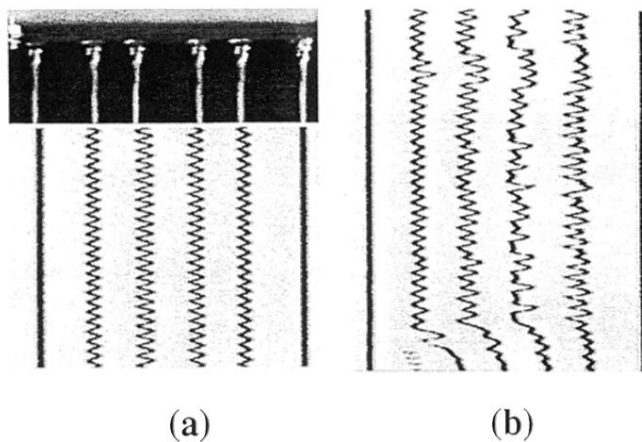
FIG. 3. (a) Oscillations of four columns. The mean wavelength λ is forced by the positions of the boundary columns. Time increases downward. (b) Chaotic oscillations observed after again increasing λ.